

## Search for the Lepton Family Number Violating Process $\bar{\nu}_\mu e^- \rightarrow \mu^- \bar{\nu}_e$

J. A. Formaggio,<sup>2</sup> J. Yu,<sup>3</sup> T. Adams,<sup>4</sup> A. Alton,<sup>4</sup> S. Avvakumov,<sup>8</sup> L. de Barbaro,<sup>5</sup> P. de Barbaro,<sup>8</sup> R. H. Bernstein,<sup>3</sup> A. Bodek,<sup>8</sup> T. Bolton,<sup>4</sup> J. Brau,<sup>6</sup> D. Buchholz,<sup>5</sup> H. Budd,<sup>8</sup> L. Bugel,<sup>3</sup> J. M. Conrad,<sup>2</sup> R. B. Drucker,<sup>6</sup> B. T. Fleming,<sup>2</sup> J. Foster,<sup>4</sup> R. Frey,<sup>6</sup> J. Goldman,<sup>4</sup> M. Goncharov,<sup>4</sup> D. A. Harris,<sup>3</sup> R. A. Johnson,<sup>1</sup> J. H. Kim,<sup>2</sup> S. Koutsoliotas,<sup>2</sup> M. J. Lamm,<sup>3</sup> W. Marsh,<sup>3</sup> D. Mason,<sup>6</sup> J. McDonald,<sup>7</sup> K. S. McFarland,<sup>8</sup> C. McNulty,<sup>2</sup> D. Naples,<sup>7</sup> P. Nienaber,<sup>3</sup> A. Romosan,<sup>2</sup> W. K. Sakumoto,<sup>8</sup> H. M. Schellman,<sup>5</sup> M. H. Shaevitz,<sup>2</sup> P. Spentzouris,<sup>3</sup> E. G. Stern,<sup>2</sup> N. Suwonjandee,<sup>1</sup> M. Vakili,<sup>1</sup> A. Vaitaitis,<sup>2</sup> U. K. Yang,<sup>8</sup> G. P. Zeller,<sup>5</sup> and E. D. Zimmerman<sup>2</sup>

<sup>1</sup>University of Cincinnati, Cincinnati, Ohio 45221

<sup>2</sup>Columbia University, New York, New York 10027

<sup>3</sup>Fermi National Accelerator Laboratory, Batavia, Illinois 60510

<sup>4</sup>Kansas State University, Manhattan, Kansas 66506

<sup>5</sup>Northwestern University, Evanston, Illinois 60208

<sup>6</sup>University of Oregon, Eugene, Oregon 97403

<sup>7</sup>University of Pittsburgh, Pittsburgh, Pennsylvania 15260

<sup>8</sup>University of Rochester, Rochester, New York 14627

(Received 16 April 2001; published 27 July 2001)

The NuTeV experiment at Fermilab has used a sign-selected neutrino beam to perform a search for the lepton number violating process  $\bar{\nu}_\mu e^- \rightarrow \mu^- \bar{\nu}_e$ , and to measure the cross section of the standard model inverse muon decay process  $\nu_\mu e^- \rightarrow \mu^- \nu_e$ . NuTeV measures the inverse muon decay asymptotic cross-section slope  $\sigma/E$  to be  $(13.8 \pm 1.2 \pm 1.4) \times 10^{-42}$  cm<sup>2</sup>/GeV. The experiment also observes no evidence for lepton number violation and places one of the most restrictive limits on the cross-section ratio  $\sigma(\bar{\nu}_\mu e^- \rightarrow \mu^- \bar{\nu}_e)/\sigma(\nu_\mu e^- \rightarrow \mu^- \nu_e) \leq 1.7\%$  at 90% C.L. for  $V-A$  couplings and  $\leq 0.6\%$  for scalar couplings.

DOI: 10.1103/PhysRevLett.87.071803

PACS numbers: 13.15.+g, 11.30.Hv, 14.60.Lm

Neutrino-lepton interactions provide an excellent tool to study the properties of the weak interaction. Such purely leptonic processes experience no interference from strong coupling terms and thus provide a direct channel to investigate the nature of the weak force. The inverse muon decay (IMD) process

$$\nu_\mu + e^- \rightarrow \mu^- + \nu_e \quad (1)$$

allows one to make an accurate determination of the vector/axial-vector ( $V-A$ ) nature of the weak interaction [1]. This process is also sensitive to scalar couplings and right-handed currents.

An experiment with separate neutrino and antineutrino beams can search for the process:

$$\bar{\nu}_\mu + e^- \rightarrow \mu^- + \bar{\nu}_e. \quad (2)$$

Such an interaction is forbidden by the standard model, since it violates lepton family number conservation ( $\Delta L_e = -\Delta L_\mu = 2$ ). Theories which incorporate multiplicative lepton number conservation [2], left-right symmetry [3], or the existence of bileptons [4] allow for such processes to occur.

The NuTeV neutrino experiment at Fermilab has investigated these processes in its high-energy, sign-selected neutrino beam line. Although the NuTeV inverse muon decay measurement is dominated by systematic uncertainties, the search for lepton number violation (LNV) processes is very sensitive because the relevant backgrounds are highly suppressed.

The experiment collected data during the 1996–1997 fixed target run, receiving a total of  $2.9 \times 10^{18}$  800-GeV protons striking a BeO target. Pions and kaons produced in the interaction were focused using the sign-selected quadrupole train (SSQT) [5] and aimed toward the NuTeV detector at a 7.8 mrad angle relative to the primary proton beam direction. The SSQT enabled the detector to be exposed to either pure neutrino or pure anti-neutrino beams. NuTeV received  $1.3 \times 10^{18}$  and  $1.6 \times 10^{18}$  protons on target for neutrino and anti-neutrino running modes, respectively. The fractional contamination from wrong-sign meson decays was below  $5 \times 10^{-3}$  [6]. Pions and kaons decay to neutrinos as they travel through a 440 m vacuum pipe; undecayed hadrons are filtered out in a beam dump at the end of the pipe. The neutrinos pass through about 900 m of earth berm shielding before reaching the NuTeV neutrino detector.

The NuTeV detector [7], located 1.4 km downstream of the primary target, consists of a segmented iron-scintillator sampling calorimeter, followed by a toroid spectrometer (see Fig. 1). The calorimeter is composed of 42 segments, each segment consisting of four 2 in. thick steel plates, two liquid scintillator counters, and one drift chamber. The calorimeter serves as a neutrino target with a fiducial mass of 350 tons. The scintillation counters measure the deposited hadronic energy and the drift chamber determine the position and direction of the outgoing muon. The toroid spectrometer uses a 15 kG toroid magnetic field to measure the charge and energy of muons exiting from

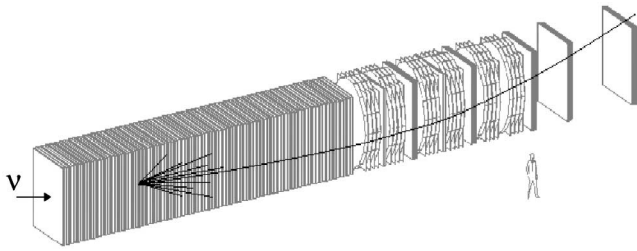


FIG. 1. Schematic of the NuTeV detector, showing the calorimeter and the toroid spectrometer.

the calorimeter. The toroid magnetic field is configured so as to always focus muons coming from the selected neutrino beam ( $\mu^-$  for neutrinos;  $\mu^+$  for antineutrinos). The energy resolution and response of the detector is measured directly using a separate beam of hadrons, muons, and electrons at varying energies. The hadronic energy resolution of the calorimeter is  $\sigma/E = (0.022 \pm 0.001) \oplus (0.86 \pm 0.01)/\sqrt{E}$ , and the electromagnetic energy resolution is  $\sigma/E = (0.042 \pm 0.002) \oplus (0.499 \pm 0.008)/\sqrt{E}$  [8], where  $E$  is measured in GeV. The resolution of the muon energy as determined by the toroid spectrometer is  $\Delta p/p = 11\%$ , limited predominantly by multiple scattering.

The selection criteria for the inverse muon decay measurement and the lepton number violation search were similar, since the characteristic signatures of the processes are nearly identical. Candidate events were selected based on the following criteria: the event occurred during the beam gate, had its interaction vertex within the fiducial volume, and had a single  $\mu^-$  reaching the toroid spectrometer. The muon was required to be well contained within the toroid and to have an energy between 15 and 600 GeV. The muon angle was also required to be less than 150 mrad with respect to the beam axis. To reduce the number of cosmic ray muons entering the selection sample, events which contained significant activity upstream of the reconstructed vertex were removed. The hadronic energy of the interaction was required to be less than 3 GeV. Finally, the neutrino beam running mode determined the sample into which the events were placed. For IMD, we required a  $\mu^-$  in the neutrino mode; for LNV candidates, a  $\mu^-$  in the antineutrino mode. For the LNV sample, we also placed an additional requirement on the  $\chi^2$  of the muon track within the toroid, in order to minimize events where the charge of the muon was misidentified.

Because both IMD and LNV events involve neutrino scattering from an electron, there exists a kinematic limit on the transverse momentum of the muon:  $p_t^2 \leq m_e E_\nu/2$ , where  $m_e$  is the mass of the electron and  $E_\nu$  is the neutrino energy. We therefore apply an energy-dependent requirement on the transverse momentum of the event in order to further isolate signal events. The cut requires  $p_t^2 \leq p_t^{2\max}$ , where  $p_t^{2\max} \equiv (0.059 + E_\mu/671) \text{ GeV}^2$ . This cut, which is based on Monte Carlo signal studies, was designed to retain 90% of the signal. The efficiency after all cuts for IMD

events was 79.6%. The final efficiency for LNV events was 89.8% for  $V-A$  couplings and 79.9% for scalar couplings. Figures 2 and 3 show the  $p_t^2$  distributions for right-sign and wrong-sign events, respectively. Right-sign events are neutrino (antineutrino) events with an outgoing  $\mu^-$  ( $\mu^+$ ); wrong-sign events are the opposite: neutrino (antineutrino) events with an outgoing  $\mu^+$  ( $\mu^-$ ).

For right-sign events, the primary backgrounds that enter the IMD sample come from low hadronic energy neutrino charged-current interactions in the detector. These include quasielastic events, resonance events, and some small fraction of deep-inelastic scattering (DIS) events with a very small momentum transfer [9,10]. Understanding the background levels is essential for the IMD measurement, since the signal to background ratio for these events is 1:8. To accomplish this, we perform a full Monte Carlo simulation of low hadronic energy neutrino processes. To simulate neutrino resonance production, we used a low- $Q^2$  higher-twist approximation [11]. We found this method more accurate in averaging over all low-multiplicity states than the single-pion production model from Rein and Sehgal [12]. Nuclear effects such as Fermi motion [13] and Pauli suppression [9,14] were also applied to the Monte Carlo simulations. The Monte Carlo (MC) was absolutely normalized to data DIS events with hadronic energies above 30 GeV for each running mode. The normalization sample contained  $0.83(0.25) \times 10^6$  neutrino (antineutrino) interactions with a mean energy of 140(120) GeV.

The dominant systematic uncertainties for the right-sign events are related to the modeling of these low hadronic energy processes. Systematic errors include effects from muon energy and angular resolution, background cross-section uncertainties, Pauli suppression, and MC normalization. In addition, we take into account radiative correction errors which affect the IMD cross section. A complete list of systematic errors is shown in Table I.

The validity of the background modeling was checked directly against the data by looking at the right-sign, antineutrino process  $\bar{\nu}_\mu + N \rightarrow \mu^+ + N'$ . This particular

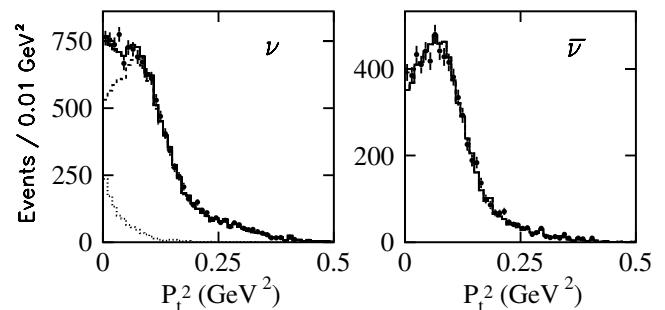


FIG. 2. Transverse momentum distributions for data (crosses) and Monte Carlo (solid line) for right-sign neutrino events (left) and right-sign antineutrino events (right). The plot on the left is broken down into background only (dashed line) and IMD signal (dotted line). The plot on the right shows Monte Carlo background only.

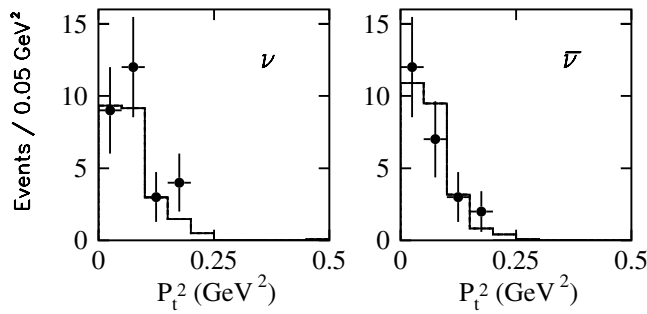


FIG. 3. Transverse momentum distributions for data (crosses) and Monte Carlo (solid line) for neutrino events (left) and antineutrino events (right) with a wrong-sign muon. A LNV signal would appear as an excess of events in the antineutrino mode.

configuration selects only background events and thus is an ideal platform to test the data to Monte Carlo agreement and systematics. A fit to the antineutrino  $p_t^2$  distribution (Fig. 2) is performed where the backgrounds are allowed to vary within the uncertainties shown in the first column of Table I. The fit gives an excellent  $\chi^2/\text{d.o.f.}$  of 44.9/50, indicating that the background estimate agrees well with the antineutrino data within the systematic uncertainties.

Having verified the size and spectrum of the background, a fit to the neutrino data is performed to extract the IMD signal. The fit includes the previously mentioned backgrounds plus an IMD signal contribution with the proper  $p_t^2$  distribution. As before, the backgrounds are allowed to vary within the uncertainties shown in the first column of Table I. As shown in Fig. 2, the data are well described by the combination of an IMD signal at low  $p_t^2$  plus the background. From the fit, we extract a total of  $1050 \pm 139$  IMD events, where 1311 events were expected based on standard model predictions, taking into account radiative corrections [15] (see Table II).

The differential cross section for IMD can be written as

$$\frac{d\sigma}{dy} = \sigma_0 \cdot E_\nu \cdot (1 - r), \quad (3)$$

TABLE I. Errors on IMD expected signal and LNV expected background. Total statistical and systematic errors reflect errors from full parameter fit, which take into account correlations between errors.

Category	IMD (%)	LNV (%)
Statistical error	$\pm 6.7$	$\pm 13.0$
Muon energy scale	$\pm 1.0$	$\pm 2.2$
Hadron energy scale	$\pm 0.3$	$\pm 0.7$
Angle smearing	$\pm 0.6$	$\pm 1.4$
Normalization	$\pm 6.4$	$\pm 2.6$
Quasielastic cross section	$\pm 1.0$	$\pm 0.6$
Pauli suppression	$\pm 8.5$	$\pm 2.2$
Beam impurities	N/A	$\pm 0.7$
Charge identity	$\ll 0.1$	$\pm 1.5$
Radiative corrections	$\pm 1.0$	$\pm 1.0$
Total systematics (fit)	$\pm 8.2$	$\pm 4.4$

where  $y = E_\mu/E_\nu$ ,  $r = m_\mu^2/s$ ,  $\sigma_0 = \frac{2m_e G_F^2}{\pi}$ , and  $s$  is the center-of-mass energy of the interaction. For inverse muon decay, the NuTeV measurement for the IMD asymptotic cross-section slope ( $E_\nu \gg m_\mu$ ) is

$$\sigma_0 = (13.8 \pm 1.2 \pm 1.4) \times 10^{-42} \text{ cm}^2/\text{GeV}, \quad (4)$$

where the first error is statistical and the second is systematic. The average neutrino energy for the IMD events sampled in the NuTeV experiment is 130 GeV. This measurement is in agreement with the theoretically predicted value of  $17.2 \times 10^{-42} \text{ cm}^2/\text{GeV}$  and is also consistent with the CHARM II measurement of  $(16.5 \pm 0.9) \times 10^{-42} \text{ cm}^2/\text{GeV}$  [16].

By requiring that the muon charge not match the neutrino running mode (wrong-sign events), the analysis immediately becomes sensitive to lepton number violation. The dominant backgrounds in this case arise from beam impurities and muon charge misidentification. Beam impurities come mainly from charmed meson decays and decays of wrong-sign hadrons produced in secondary interactions [17]. Beam impurities constitute about 72% of the total LNV background. Charge misidentification backgrounds are often associated with  $\delta$ -ray production or multiple scattering of the muon in the toroid spectrometer. These backgrounds can be greatly reduced by imposing quality cuts on the muon track in the toroid spectrometer. The total fraction of charge misidentification is 0.06% for the antineutrino running mode. This source contributes 14% of the LNV background. Finally, there exists an irreducible background from  $\bar{\nu}_e e^- \rightarrow \mu^- \bar{\nu}_\mu$ , which contributes about 14% of the LNV background.

The generic expression for the differential LNV cross section is given by

$$\frac{d\sigma}{dy} = \lambda \frac{G_F^2 s}{\pi} [A_V \cdot y(y - r) + A_S(1 - r)], \quad (5)$$

where  $\lambda$  represents the strength of the interaction and  $A_V$  and  $A_S$  determine whether the reaction is  $V-A$  or scalar. Integrating over all allowed values of  $y$ , and normalizing to the standard model IMD cross section, allows the LNV cross section to be written as

$$\frac{\sigma(\bar{\nu}_\mu e^- \rightarrow \mu^- \bar{\nu}_e)}{\sigma(\nu_\mu e^- \rightarrow \mu^- \nu_e)} = \lambda \left[ A_V \left( \frac{1 + r/2}{3} \right) + A_S \right]. \quad (6)$$

We can make a consistency check on the background estimation by looking at the neutrino process  $\nu_\mu + N \rightarrow \mu^+ + N'$ . Momentum distributions of these events are

TABLE II. Signal extraction from Monte Carlo background.

Type	$\nu$ Mode/ $\mu$ Charge	Data	Fit results
IMD signal	$\nu/\mu^-$	11 792	$1050 \pm 139$
LNV signal ( $V-A$ )	$\bar{\nu}/\mu^-$	24	$0.6 \pm 3.3$
LNV signal (scalar)	$\bar{\nu}/\mu^-$	24	$-0.6 \pm 3.3$

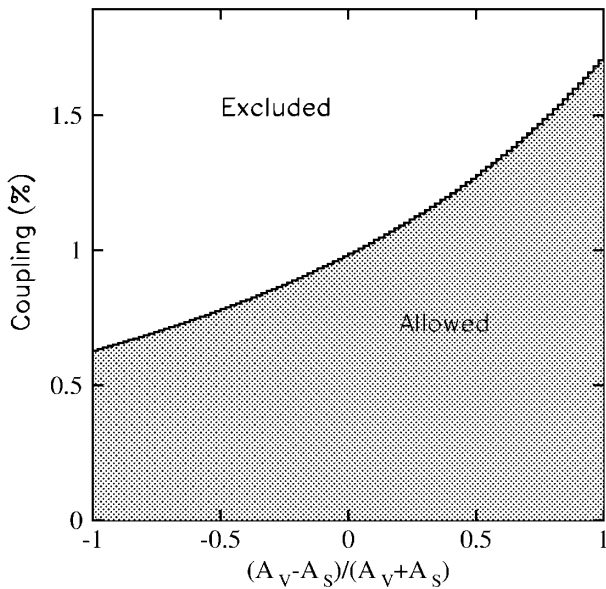


FIG. 4. Limit on the lepton number violation process  $\bar{\nu}_\mu e^- \rightarrow \mu^- \bar{\nu}_e$  as a function of the scalar and vector couplings  $(A_V - A_S)/(A_V + A_S)$ . The nonshaded region is excluded by this result.

shown in Fig. 3. A total of 28 data events were seen in this sample where  $23.5 \pm 3.7$  (stat + syst) were expected, consistent with the background estimate.

Looking in the LNV signal channel  $\bar{\nu}_\mu + e^- \rightarrow \mu^- + \bar{\nu}_e$  yields a total of 24 data events. A fit of the  $p_i^2$  distribution to only background sources yields an acceptable  $\chi^2/\text{d.o.f.}$  of 2.5/5, showing no indication of a LNV signal. Including a possible LNV signal in the fit yields a total LNV contribution of  $0.6 \pm 3.1 \pm 1.1$  events for a  $V$ - $A$  coupling and  $-0.6 \pm 3.1 \pm 1.1$  events for a scalar coupling. As shown in Table I, the LNV analysis is dominated by statistical uncertainty. These fit results can be recast in the form of 90% C.L. limits on the LNV cross section as a function of  $(A_V - A_S)/(A_V + A_S)$ , as shown in Fig. 4. If we assume a pure  $V$ - $A$  coupling, this yields  $\lambda \leq 1.7\%$  while a scalar coupling yields a limit of  $\lambda \leq 0.6\%$ .

This limit is currently the most stringent limit obtained directly from neutrino-electron scattering. Previous results limited the pure  $V$ - $A$  coupling to below 5% [18]. The LAMPF experiment has set an earlier limit from muon decay rates at  $\leq 1.2\%$  [19] for pure  $V$ - $A$  couplings. Improved model-dependent limits on family lepton number violation can also be obtained from muonium-antimuonium experiments [20,21].

In conclusion, NuTeV has performed a measurement of the inverse muon decay cross section and a direct search for lepton number violation. The IMD asymptotic cross-section slope is measured to be  $(13.8 \pm 1.2 \pm 1.4) \times 10^{-42} \text{ cm}^2/\text{GeV}$ . The LNV search limits the strength of the interaction to be  $\leq 1.7\%$  for  $V$ - $A$  and  $\leq 0.6\%$  for scalar couplings.

This research was supported by the U.S. Department of Energy and the National Science Foundation. We thank the staff of FNAL for their contributions to the construction and support of this experiment during the 1996–1997 fixed target run.

- 
- [1] W. Fetscher, H. J. Gerber, and K. F. Johnson, Phys. Lett. B **173**, 102 (1986).
  - [2] G. Feinberg and S. Weinberg, Phys. Rev. Lett. **6**, 381 (1961).
  - [3] P. Herczeg and R. N. Mohapatra, Phys. Rev. Lett. **69**, 2475 (1992).
  - [4] F. Cuypers and S. Davidson, Eur. Phys. J. C **2**, 503 (1998).
  - [5] J. Yu *et al.*, "Technical Memorandum: NuTeV SSQT performance," Fermilab Report No. FERMILAB-TM-2040, 1998.
  - [6] A. Alton *et al.*, Phys. Rev. D **63**, 012001 (2001).
  - [7] W. Sakumoto *et al.*, Nucl. Instrum. Methods Phys. Res., Sect. A **294**, 179 (1990); B. King *et al.*, Nucl. Instrum. Methods Phys. Res., Sect. A **302**, 254 (1991).
  - [8] D. A. Harris *et al.*, Nucl. Instrum. Methods Phys. Res., Sect. A **447**, 377 (2000).
  - [9] C. H. Llewellyn Smith, Phys. Rep. **3C**, 261 (1971).
  - [10] R. Belusevic and D. Rein, Phys. Rev. D **46**, 3747 (1992).
  - [11] U. K. Yang and A. Bodek, Phys. Rev. Lett. **82**, 2467 (1999).
  - [12] D. Rein and L. M. Sehgal, Ann. Phys. (N.Y.) **133**, 79 (1981).
  - [13] A. Bodek and J. L. Ritchie, Phys. Rev. D **23**, 1070 (1981).
  - [14] E. A. Paschos, L. Pasquali, and J. Y. Yu, Nucl. Phys. **B588**, 263 (2000).
  - [15] D. Yu. Bardin and V. A. Dokuchaeva, Nucl. Phys. **B287**, 839 (1987).
  - [16] P. Vilain *et al.*, Phys. Lett. B **364**, 121 (1995).
  - [17] A. Alton, Ph.D. thesis, Kansas State University, 2001; A. Alton *et al.*, hep-ex/0008068 [Phys. Rev. D (to be published)].
  - [18] F. Bergsma *et al.*, Phys. Lett. **122B**, 465 (1983).
  - [19] S. J. Freedman *et al.*, Phys. Rev. D **47**, 811 (1993).
  - [20] L. Willmann *et al.*, Phys. Rev. Lett. **82**, 49 (1999).
  - [21] S. Bergmann and Y. Grossman, Phys. Rev. D **59**, 093005 (1999).